1028

NEANDC (E) 204 "L"
INDC (FR) 34/L

CALCULATION OF ^{232}Th NEUTRON CROSS SECTIONS FROM 0.3 MeV TO 2.4 MeV INCLUDING A FISSION CHANNEL ANALYSIS

H. ABOU YEHIA, J. JARY, J. TROCHON

Service de Physique Nucléaire
Centre d'Etudes de Bruyères-le-Châtel
B.P. n° 561
92542 MONTROUGE CEDEX, France

- MARS 1979 -

COMMISSARIAT A L'ENERGIE ATOMIQUE
FRANCE

NEANDC (E) 204 "L"
INDC (FR) 34/L

CALCULATION OF ^{232}Th NEUTRON CROSS SECTIONS FROM 0.3 MeV TO 2.4 MeV INCLUDING A FISSION CHANNEL ANALYSIS.

by

H. ABOU YEHIA, J. JARY, J. TROCHON

Service de Physique Nucléaire
Centre d'Etudes de Bruyères-le-Châtel
B.P. n° 561
92542 MONTROUGE CEDEX, France

- MARCH 1979 -

CALCULATION OF ^{232}Th NEUTRON CROSS SECTIONS FROM 0.3 MeV TO 2.4 MeV INCLUDING A FISSION CHANNEL ANALYSIS

ABSTRACT -

In this report, we present a consistent calculation of all the neutron cross sections - total, elastic and inelastic scattering, radiative capture and fission - of ^{232}Th in the neutron energy range 0.3 - 2.4 MeV. The experimental fission cross sections and fragment angular distributions are fairly reproduced by a channel analysis method.

CALCUL DES SECTIONS EFFICACES NEUTRONIQUES DE ^{232}Th DE 0.3 MeV A 2.4 MeV AVEC UNE ANALYSE EN VOIES DE FISSION

RESUME -

Nous présentons dans ce rapport un calcul coherent des sections efficaces neutroniques - totale, diffusion élastique et inélastique, capture radiative et fission - de ^{232}Th pour des neutrons d'énergie comprise entre 0.3 et 2.4 MeV. Les données expérimentales sur la section efficace de fission et les distributions angulaires des fragments sont bien reproduites par une méthode d'analyse en voies de sortie de fission.

I - INTRODUCTION -

Among the different studies of the fission process, the fission of thorium isotopes is probably one of the most interesting at the present time. Such a study has begun by the neutron induced fission of ^{232}Th which is the easier thorium isotope to obtain. A large amount of experimental data on this nucleus is now available.

The ^{232}Th(n,f) cross section in the threshold region exhibits large and well separated resonances, associated with important fluctuations in the fission fragment angular distributions [1-2-3]. In the framework of the MÖLLER and NIX calculations [4], these resonances are interpreted as vibrational states in a third well of the fission barrier. In addition, a fine structure seems to be superimposed to these resonances, but their interpretation differs following the authors [1-5]. The fission fragment characteristics also present interesting properties. In particular, a recent measurement of the mean total kinetic energy seems to reveal a fission process behaviour for ^{232}Th different from that for other actinides, and leads to a search for channel effects in this nucleus [6].

The interpretation of these different data requires the knowledge of the transition states of the nucleus. Informations on these states can be obtained from a simultaneous analysis of the experimental fission cross section and fragment angular distributions. Up to now, different attempts using double or triple humped fission barriers have been made but rarely any detailed calculation of the other neutron cross sections, thus preventing a check of the consistency of the calculation.

In this paper, we report a simultaneous analysis of all the cross sections of ^{232}Th - total, elastic and inelastic scattering, radiative capture, fission - and the fission fragment angular distributions in the neutron energy range 0.3 - 2.4 MeV.

II - DESCRIPTION OF THE MODEL -

The calculation of the Hauser-Feshbach type used a code based on the statistical model [7]. In this model, the interaction of a neutron with a target nucleus (spin I) leads to the formation of a compound nucleus which can de-excite by gamma-ray emission, neutron emission or fission. The nuclear reaction cross section can be written [7]

$$\sigma_{cc'}(E_n) = \sum_{J\pi} \sigma_c(E, J, \pi)\ P_{c'}(E, J, \pi)$$

where c and c' label the entrance and exit channels respectively. E_n is the incident neutron energy. $P_{c'}(E, J, \pi)$ is the branching ratio of the compound nucleus state (E, J, π) to the channel c' with corrections due to width fluctuations. The quantities E, J, π denote respectively the excitation energy, spin and parity of this state.

In this study, the compound nucleus formation cross section $\sigma_c(E, J, \pi)$ makes use of the neutron penetrabilities obtained from a coupled channel calculation performed by Lagrange [8]. The parametrisation of the deformed optical potential used in this calculation is described in reference [9]. It gives satisfactory values of the s and p wave strength functions calculated at 10 keV, i.e. respectively $S_o = 1.005\ 10^{-4}$ and $S_1 = 1.518\ 10^{-4}$. The total cross section σ_T calculated at low energy by this model is plotted and compared with the experimental data [10-11-12] in fig.1. In spite of a slight difference ($\leqslant 7$ %) between 1 and 1.8 MeV, the agreement is generally good.

The branching ratios $P_{c'}(E, J, \pi)$ are related to the transmission coefficients $T_{c'}(E, J, \pi)$ associated to the exit channel c' by

$$P_{c'}(E, J, \pi) = \frac{T_{c'}(E, J, \pi)}{\sum_{c''} T_{c''}(E, J, \pi)}$$

For fission, the exit channels (or transition states) are characterized by the quantum number K (projection of the total angular momentum J on the symmetry axis of the nucleus). The fission transmission coefficients $T_f(E, J, K, \pi)$ are calculated [7] by numerical integration of a Shrödinger type equation. The fission

barriers used are triple humped, according to Möller and Nix calculations [4] and Blons experimental results [1]. As the first hump top located at about 4 MeV does not influence the barrier penetrability in the energy range studied, the penetrabilities can be calculated in the framework of a double humped barrier consisting of the second and third humps. Always in agreement with the former works [1-4], the third well is assumed shallow enough so that damping of the vibrational states of this well into the other intrinsic states is negligible.

As a consequence of the axially deformed nature of the third well, each vibrational state is assumed to be splitted into two states weakly separated (by about 10 keV) having the same barrier shape and the same number K but opposite parities.

If one assumes that the fission fragments separate along the nucleus symmetry axis and K is a good quantum number, the fission fragment angular distribution of an even-even target nucleus as ^{232}Th for a particular transition state is given by

$$W^{J}_{\pm 1/2,\, \pm K}(\theta) = \frac{2J+1}{4} \left[|d^{J}_{1/2,\, K}(\theta)|^2 + |d^{J}_{-1/2,\, K}(\theta)|^2 \right]$$

where $d^{J}_{\pm 1/2, K}(\theta)$ is the rotational part of the symmetric top wave function. θ denotes the angle between the symmetry axis of the nucleus and the direction of the incident neutrons.

For all the transition states, the fission fragment angular distribution and the fission cross section are given respectively by the relations

$$W(\theta,E) = \sum_{J,K,\pi} \sigma_f(E,J,K,\pi)\, W_{\pm 1/2,\, \pm K}(\theta)$$

$$\sigma_f(E) = \sum_{J,K,\pi} \sigma_f(E,J,K,\pi)$$

The neutron transmission coefficients $T_n(E,J,\pi)$ are sums over all the contributions of neutron channels leaving the target nucleus in its ground state or in an

excited state λ (having spin I_λ and parity Π_λ).

$$T_n(E, J, \pi) = \sum_{\lambda} \sum_{j'=|J-I_\lambda|}^{J+I_\lambda} \sum_{\ell'=j'-1/2}^{j'+1/2} T_{\ell'}^{j'}(E-E_\lambda)\delta_{\pi, \ell'+\pi_\lambda}$$

$$+ 1/2 \sum_{\lambda} \sum_{j'=|J-I_\lambda|}^{J+I_\lambda} \sum_{\ell'=j'-1/2}^{j'+1/2} \int_0^{E-E_\lambda} \rho_{I_\lambda}(E-\varepsilon)\, T_{\ell'}^{j'}(\varepsilon)d\varepsilon$$

where T_ℓ^j is the common neutron penetrability and $\rho(E)$ a continuum level density.

The excited states λ used in this calculation are listed in table I. Above 1.12 MeV, the conventional Fermi-gas formula of Gilbert and Cameron [13] $\left(\rho(E) = \frac{1}{T} \exp\left(\frac{E-E_0}{T}\right)\right)$ has been used. Its parameters obtained from an adjustment to the experimental data (mean level spacing at the neutron resonance energies, D_{obs} = 17.49 eV and discrete level scheme fig.2) are E_x = 5.1 MeV, E_0 = - 0.2 MeV, T = 0.399 MeV.

The radiative capture transmission coefficients $T_\gamma(E, J, \pi)$ are related to the average capture widths $\overline{\Gamma}_\gamma$ by

$$T_\gamma(E, J, \pi) = 2\pi\, \rho(E_c, J, \pi)\, \overline{\Gamma}_\gamma(E_c)$$

where $\rho(E_c, J, \pi)$ denotes the Fermi-gas level density [13] of the compound nucleus ^{233}Th in its state (E_c, J, π). The γ-ray widths have been calculated according to the Weisskopf formalism [14] and normalized to the experimental value Γ_γ^{exp}(21.2 meV [14]) measured at the neutron resonance energies.

III - RESULTS -

The computational procedure consisted of adjusting the heights (E_B, E_{III}, E_c) and widths ($\hbar\omega_B$, $\hbar\omega_{III}$, $\hbar\omega_c$) of the fission barriers corresponding to each state ($K\pi$), in order to obtain simultaneously a good fit to the experimental fission

cross sections as well as fragment angular distributions. A set of 28 fission channels was needed. They are listed in table II.

All the neutron cross sections calculated in this work are reported in table III and IV.

The calculated fission cross section is compared in fig.3 a,b to the experimental data [1-16]. For incident neutron energies E_n lower than 2.2 MeV, a good agreement is obtained. However for $E_n > 2.2$ MeV we were led to increase the continuous level density of ^{232}Th by about a factor 2 in order to achieve the fit. This means an increased neutron scattering competition in this energy range, which remains until now an open question.

The fragment angular distribution results corrected for the neutron energy resolution are compared in fig.4 to the experimental data [2-3]. Another detailed calculation between 1.57 MeV and 1.62 MeV by energy steps of 4 keV has been carried out to search for the experimentally observed fine structures [1]. As can be seen in fig.5, our calculated fission cross section does not exhibit any fine structure superimposed on the broad vibrational resonance at $E_n = 1.6$ MeV. Notwithstanding a good agreement between calculated and experimental [5] fission fragment angular distributions is obtained (fig.6).

The scattering and radiative capture cross sections are given in fig.7, 8 and 9. The calculated elastic and inelastic cross sections reproduce satisfactorily the experimental data [17-18-19-20]. The slight disagreement for the partial inelastic cross sections associated to the levels at 49.37 keV and 162.1 keV is mainly due to the 5 % discrepancy between calculated and measured total cross sections below $E_n = 2$ MeV (see fig.1). The radiative capture data [15-21-17-22-23-24] are well reproduced over all the studied energy range in particular the structure below $E_n = 1$ MeV.

IV - CONCLUSION -

All the ^{232}Th neutron cross sections have been satisfactorily reproduced in a consistent way in the large energy range considered in this work. However the following remarks must be pointed out :

i) The set of the fission channels listed in table II fairly reproduce the fission characteristics in the framework of our calculations. We do not claim that it is unique.

ii) The fission fragment angular distributions as well as the vibrational resonances in the fission cross sections are generally well reproduced. But, around E_n = 1.6 MeV, the fine structures observed experimentally are not seen in these calculations whereas the calculated fission fragment angular distributions are in good agreement with the experiment [5] (see fig.6). Our calculation does not reveal fine structures, so the observed structures could be due to another physical phenomenon not taken into account explicitly in our work.

iii) The assumption of an increased inelastic scattering competition above E_n = 2.2 MeV remains for us an open question.

This work shows that an optical statistical model conveniently adjusted on the fission characteristics can be used with confidence to generate a coherent set of neutron cross sections for a same target within a large energy range. Thus such a sort of analysis would be of interest for neighbouring nuclei if fission data are available.

REFERENCES

[1] - J. BLONS, C. MAZUR and D. PAYA, *Phys. Rev. Lett., Vol.35 (1975) 1749 and Note CEA-N-1959.*

[2] - S.B. ERMAGAMBETOV and G.N.SMIRENKIN, *Sov. J. of Nucl. Phys. Vol.11 (1970) 646.*

[3] - J. CARUANA, J.W. BOLDEMAN and R.L. WALSH, *Nucl. Phys. A285 (1977) 205.*

[4] - P. MÖLLER and J.R. NIX, Physics and Chemistry of fission, *IAEA Vienna I (1974) 103.*

[5] - G. BARREAU, *Thèse d'Etat (Université de Bordeaux 1977).*

[6] - J. TROCHON, H. ABOU YEHIA, F. BRISARD and Y. PRANAL, *to be published in Nucl. Phys.*

[7] - P. THOMET, Commissariat à l'Energie Atomique, *Report CEA-R-4631 (1974).*
J. JARY, Ch. LAGRANGE and P. THOMET, *Report INDC(FR) 9/L - NEANDC(E) 174 "L" (1977).*

[8] - Ch. LAGRANGE, *Private communication.*

[9] - G. HAOUAT, J. LACHKAR, Ch. LAGRANGE, Y. PATIN, J. SIGAUD, R.E. SHAMU, *Report NEANDC(E) 196"L", INDC(FR) 29/L (1978).*

[10] - L. GREEN et al., *BNL-325, third edition, Vol.II (1971).*

[11] - U. FASOLI, D. TONIOLO, G. ZAGO and I.ZUFFI *Nucl. Phys. A151 (1970) 369.*

[12] - J. WAHLEN and A.B. SMITH, *Nucl. Sc. Eng. 67 (1978) 129.*

[13] - A. GILBERT and A.G.W. CAMERON, *Can. J. Phys. 43 (1965) 1446.*

[14] - J.M. BLATT, and V.F. WEISSKOPF, *Theoretical Nuclear Physics, Ed. Wiley (1952).*

[15] - G. de SAUSSURE and R.L. MACKLIN, *ORNL/TM-6161 (1977).*

[16] - J.W. BEHRENS and J.C. BROWNE, *Phys. Lett. Vol. 69B (1977) 278.*

[17] - J. MEADOWS, W. POENITZ, A.SMITH, D. SMITH, and J. WHALEN, *ANL/NDM-35 (1978).*

[18] - W. McMURRAY, *Report SUNI-41 (1975).*

[19] - A. SMITH, *Phys. Rev. 126 (1962) 718.*

[20] - G. HAOUAT, J. SIGAUD, J. LACHKAR, Ch. LAGRANGE, B. DUCHEMIN, and Y. PATIN, *Report INDC(FR) 13/L - NEANDC(E) 180 "L" (1977).*

[21] - M. LINDNER, R.J. NAGLE and J.H. LANDRUM, *Nucl. Sc. Eng.* 59 *(1976) 381 - See also Ref. 14.*

[22] - H.M. JAIN, H.P. ANAND, M.L. JHINGAN, R.N. JINDAL, V.C. DENIZ and M.K. MEHTA, *Int. Conf. on Neutron Physics (HARWELL 1978).*

[23] - J.A. MISKEL, K.V. MARSH, M. LINDNER and R.J. NAGLE, *Phys. Rev.* 128 *(1962) 2717 - See also ref. 14.*

[24] - J.F. BARRY, L.P. O'CONNOR and J.L. PERKIN, *Proc. Phys. Soc. (London)* 74 *(1959) 685.*

TABLE CAPTIONS

Table I : Excited levels of ^{232}Th used in the calculation of the scattering competition.

Table II : Parameters corresponding to the set of transition states (K,π) needed to fit the fission cross section and the fragments angular distributions. E_B, E_{III}, E_c are the heights of the second hump, third well and third hump in the potential barrier respectively. $\hbar\omega_B$, $\hbar\omega_{III}$, $\hbar\omega_c$ are the corresponding widths.

Table III : Calculated partial inelastic scattering cross sections to the different ^{232}Th excited levels.

Table IV : Calculated total elastic scattering, radiative capture and fission cross sections.

LEVEL	ENERGY (MeV)	SPIN	PARITY
0	0.0	0	+
1	0.049369	2	+
2	0.16212	4	+
3	0.33310	6	+
4	0.55690	8	+
5	0.71425	1	-
6	0.73035	0	+
7	0.77410	2	+
8	0.77440	3	-
9	0.78520	2	+
10	0.82740	10	+
11	0.82960	3	+
12	0.87300	4	+
13	0.88330	5	-
14	0.89010	4	-
15	0.96020	4	+
16	1.05360	2	-
17	1.0729	2	+
18	1.0775	1	-
19	1.0787	0	+
20	1.0944	3	+
21	1.1057	3	-
22	1.1228	2	+

TABLE I

(k,π) state	E_B (MeV)	E_{III} (MeV)	E_C (MeV)	$\hbar\omega_B$ (MeV)	$\hbar\omega_{III}$ (MeV)	$\hbar\omega_C$ (MeV)
$\frac{1}{2}^+$	5.49	5.47	6.86	1.30	0.60	1.30
$\frac{7}{2}^-$	5.70	5.46	6.875	0.74	0.60	1.05
$\frac{1}{2}^+$	6.27	5.72	6.86	1.20	1.0	1.23
$\frac{3}{2}^+$	6.29	5.723	6.77	1.4	1.0	1.40
$\frac{1}{2}^+$	6.22	5.86	7.24	1.4	1.0	1.40
$\frac{3}{2}^+$	6.35	5.81	6.92	1.4	1.0	1.40
$\frac{3}{2}^+$	6.62	5.90	7.01	1.4	1.0	1.40
$\frac{3}{2}^-$	6.61	5.89	7.00	1.4	1.0	1.40
$\frac{5}{2}^+$	6.45	5.90	6.96	1.4	1.0	1.40
$\frac{5}{2}^-$	6.46	5.91	6.97	1.4	1.0	1.40
$\frac{1}{2}^+$	6.73	6.026	7.62	1.4	1.0	1.40
$\frac{1}{2}^-$	6.74	6.036	7.63	1.4	1.0	1.40
$\frac{3}{2}^+$	6.78	6.016	7.29	1.4	1.0	1.40
$\frac{3}{2}^-$	6.79	6.026	7.30	1.4	1.0	1.40
$\frac{1}{2}^+$	6.76	6.19	7.43	1.4	1.0	1.40
$\frac{1}{2}^-$	6.77	6.20	7.44	1.4	1.0	1.40
$\frac{5}{2}^+$	6.85	6.175	7.23	1.4	1.0	1.40
$\frac{5}{2}^-$	6.86	6.185	7.24	1.4	1.0	1.40
$\frac{1}{2}^+$	7.01	6.305	7.54	1.4	1.0	1.40
$\frac{1}{2}^-$	7.02	6.315	7.55	1.4	1.0	1.40
$\frac{1}{2}^+$	7.20	6.38	7.70	1.4	1.0	1.40
$\frac{1}{2}^-$	7.21	6.39	7.71	1.4	1.0	1.40
$\frac{1}{2}^+$	7.20	6.48	7.54	1.4	1.0	1.40
$\frac{1}{2}^-$	7.21	6.49	7.55	1.4	1.0	1.40
$\frac{1}{2}^+$	7.22	6.55	7.57	1.4	1.0	1.40
$\frac{1}{2}^-$	7.23	6.56	7.58	1.4	1.0	1.40
$\frac{1}{2}^+$	7.24	6.625	7.52	1.4	1.0	1.40
$\frac{1}{2}^-$	7.24	6.735	7.55	1.4	1.0	1.40

TABLE II

TABLE III

CALCULATED PARTIAL INELASTIC SCATTERING CROSS SECTIONS (BARN)

Neutron Energy (MeV)	DISCRETE LEVELS (ENERGIES ARE IN MeV)						
	0.049369 2^+	0.1621 4^+	0.3331 6^+	0.5569 8^+	0.71425 1^-	0.73035 0^+	0.7741 2^+
0.150	0.50115						
0.200	0.6083						
0.250	0.7813	0.003122					
0.300	0.845	0.068					
0.400	0.920	0.030					
0.500	0.975	0.055					
0.700	1.08	0.210	$0.5626.10^{-3}$				
0.800	0.980	0.245	0.1207(-2)	0.	0.16058	0.600(-1)	0.056124
0.950	0.838	0.262	0.8417(-2)	0.	0.22549	0.1005	0.17017
1.0	0.805	0.268	0.9674(-2)	0.	0.2333	0.10474	0.19451
1.10	0.742	0.278	0.012862	0.8307(-5)	0.22859	0.10319	0.21204
1.15	0.705	0.278	0.014325	0.118(-4)	0.21763	0.098623	0.20854
1.20	0.672	0.275	0.015943	0.1627(-4)	0.20834	0.094199	0.20549
1.25	0.648	0.275	0.018174	0.2189(-4)	0.20047	0.090928	0.20293
1.30	0.625	0.272	0.019689	0.2842(-4)	0.18992	0.0859	0.19994
1.35	0.600	0.272	0.021245	0.3604(-4)	0.17901	0.081101	0.19386
1.40	0.588	0.272	0.022599	0.4450(-4)	0.16897	0.076715	0.18748
1.45	0.577	0.271	0.024121	0.5446(-4)	0.16320	0.073584	0.18421
1.50	0.568	0.270	0.025704	0.1133(-3)	0.15630	0.07007	0.17945
1.55	0.555	0.268	0.029721	0.5888(-3)	0.14699	0.065908	0.17106
1.60	0.547	0.265	0.03015	0.6378(-3)	0.13993	0.06257	0.16468
1.65	0.539	0.263	0.03131	0.7058(-3)	0.13418	0.059864	0.16066
1.70	0.53	0.260	0.03223	0.7998(-3)	0.12685	0.05658	0.15457
1.80	0.518	0.252	0.03355	0.9699(-3)	0.11453	0.05117	0.14412
1.90	0.507	0.245	0.03387	0.1113(-2)	0.10152	0.04556	0.13096
2.00	0.495	0.235	0.03355	0.126(-2)	0.09010	0.04076	0.12007
2.10	0.472	0.220	0.02821	0.1423(-2)	0.07143	0.03262	0.09686
2.20	0.450	0.205	0.02282	0.128(-2)	0.05422	0.02498	0.07476
2.30	0.430	0.180	0.01793	0.112(-2)	0.03964	0.01844	0.05604
2.40	0.410	0.154	0.01344	0.960(-3)	0.02817	0.01310	0.04017

TABLE III (Continued)

Neutron Energy (MeV)	DISCRETE LEVELS (ENERGIES ARE IN MeV)							
	0.7744 3^-	0.7852 2^+	0.8274 10^+	0.8296 3^+	0.8730 4^+	0.8833 5^-	0.8901 4^-	0.9602 4^+
0.150								
0.200								
0.250								
0.300								
0.400								
0.500								
0.700								
0.800	0.026057	0.038984						
0.950	0.093419	0.16059	0.	0.0760	0.015034	0.1124(-2)	0.020875	
1.0	0.11282	0.18637	0.	0.09422	0.024741	0.2265(-2)	0.030273	0.6349(-2)
1.10	0.13026	0.20624	0.	0.12277	0.04433	0.6711(-2)	0.046267	0.024517
1.15	0.13054	0.20344	0.	0.12707	0.05045	0.8763(-2)	0.050118	0.031911
1.20	0.13174	0.20092	0.	0.12997	0.055831	0.010873	0.053869	0.040459
1.25	0.13321	0.19879	0.	0.13271	0.060363	0.0129	0.056825	0.046659
1.30	0.13487	0.19644	0.	0.13323	0.063505	0.014752	0.058721	0.050765
1.35	0.13317	0.19066	0.	0.13643	0.066367	0.016606	0.060428	0.054277
1.40	0.13032	0.18472	0.	0.13547	0.07146	0.019542	0.06325	0.05714
1.45	0.13067	0.18161	0.	0.13633	0.07422	0.021355	0.065182	0.060277
1.50	0.12975	0.17715	0.	0.13585	0.07632	0.02325	0.066745	0.0653
1.55	0.12528	0.16892	0.	0.13164	0.07686	0.02555	0.06641	0.066533
1.60	0.12197	0.16280	0.	0.12845	0.07633	0.02632	0.06591	0.06658
1.65	0.12077	0.15886	0.	0.12784	0.07776	0.02782	0.06687	0.06841
1.70	0.11793	0.15297	0.	0.12521	0.07803	0.02894	0.06681	0.06907
1.80	0.11215	0.14282	0.496(-6)	0.12061	0.07805	0.03089	0.06645	0.06962
1.90	0.10345	0.12980	0.761(-6)	0.11251	0.07537	0.03129	0.06370	0.06808
2.00	0.09632	0.11901	0.113(-5)	0.10580	0.07304	0.03158	0.06112	0.05570
2.10	0.07785	0.09615	0.138(-5)	0.08687	0.06107	0.02712	0.05069	0.05570
2.20	0.06028	0.07422	0.157(-5)	0.06783	0.04859	0.02312	0.04010	0.0449
2.30	0.04533	0.05573	0.170(-5)	0.05158	0.03751	0.01744	0.03072	0.03475
2.40	0.03282	0.03995	0.784(-5)	0.03766	0.02808	0.0135	0.02304	0.02609

TABLE III (Continued)

Neutron Energy (MeV)	DISCRETE LEVELS (MeV)							
	1.0536 2^-	1.0729 2^+	1.0775 1^-	1.0787 0^+	1.0944 3^+	1.1057 3^-	1.1228 2^+	Continuum
0.150								
0.200								
0.250								
0.300								
0.400								
0.500								
0.700								
0.800								
0.950								
1.0								
1.10	0.036504	0.025398	0.027536	0.01105	0.5344(-2)			
1.15	0.056834	0.050608	0.052455	0.022728	0.023857	0.0202	0.02174	0.3623(-2)
1.20	0.070307	0.069118	0.067917	0.030579	0.038967	0.033439	0.044463	0.020326
1.25	0.080869	0.083464	0.078313	0.035951	0.050895	0.043357	0.061654	0.047732
1.30	0.090288	0.095331	0.086645	0.039898	0.06236	0.050899	0.074259	0.082989
1.35	0.094798	0.10219	0.089966	0.041689	0.069642	0.059326	0.085333	0.12625
1.40	0.09627	0.10620	0.091336	0.042607	0.075333	0.063672	0.091854	0.17603
1.45	0.09963	0.11003	0.093254	0.04308	0.079994	0.068121	0.097630	0.23593
1.50	0.10144	0.11215	0.093686	0.042887	0.083412	0.071392	0.10073	0.30088
1.55	0.10050	0.11113	0.092157	0.041996	0.083842	0.072097	0.10076	0.36839
1.60	0.10077	0.11197	0.09157	0.04178	0.08649	0.07319	0.1013	0.43718
1.65	0.10084	0.11213	0.09031	0.040948	0.08832	0.07623	0.10373	0.52053
1.70	0.09869	0.11018	0.08753	0.03953	0.08857	0.07654	0.1026	0.60323
1.80	0.09514	0.10665	0.0827	0.03709	0.08826	0.07644	0.1002	0.78495
1.90	0.08868	0.09979	0.07578	0.0339	0.08487	0.07343	0.094514	0.96361
2.00	0.08246	0.09335	0.06908	0.03085	0.08177	0.07037	0.08881	1.1611
2.10	0.06755	0.07689	0.05626	0.02532	0.06820	0.05866	0.07361	1.4982
2.20	0.05268	0.060252	0.04342	0.01968	0.05412	0.04632	0.05785	1.8274
2.30	0.03997	0.04597	0.032636	0.014911	0.041816	0.03556	0.04415	2.1381
2.40	0.02917	0.03364	0.02364	0.01082	0.03112	0.02646	0.03254	2.406

TABLE IV

Neutron Energy (MeV)	Total elastic Cross Section (barn)	Total inelastic cross section (barn)	Radiative Capture Cross Section (barn)	Fission Cross Section (barn)
0.3	8.34	0.84	0.134	0.
0.4	7.29	0.95	0.130	0.
0.5	6.54	1.03	0.133	0.
0.6	6.06	1.18	0.153	0.
0.7	5.54	1.29	0.165	$0.511\ 10^{-4}$
0.8	4.92	1.56	0.150	$0.165\ 10^{-3}$
0.9	4.46	1.80	0.136	$0.462\ 10^{-3}$
0.95	4.28	1.88	0.128	$0.927\ 10^{-3}$
1	4.17	2.06	0.125	$0.155\ 10^{-2}$
1.1	3.89	2.26	0.117	$0.301\ 10^{-2}$
1.15	3.77	2.37	0.113	$0.370\ 10^{-2}$
1.20	3.68	2.47	0.107	$0.462\ 10^{-2}$
1.25	3.60	2.55	0.104	$0.660\ 10^{-2}$
1.28	3.55	2.6	0.102	$0.918\ 10^{-2}$
1.30	3.53	2.62	0.101	0.0124
1.32	3.50	2.64	0.099	0.0180
1.35	3.48	2.68	0.097	0.0349
1.37	3.44	2.7	0.096	0.0518
1.40	3.43	2.72	0.095	0.0643
1.42	3.415	2.74	0.094	0.0602
1.45	3.41	2.79	0.093	0.0547
1.475	3.40	2.82	0.0928	0.0566
1.50	3.40	2.85	0.0923	0.0596
1.525	3.395	2.86	0.0915	0.0661
1.55	3.395	2.87	0.090	0.0903
1.575	3.395	2.88	0.089	0.130
1.6	3.390	2.9	0.088	0.127
1.625	3.3375	2.93	0.0875	0.0962
1.650	3.337	2.96	0.087	0.0766
1.675	3.3375	2.98	0.0865	0.0712
1.7	3.338	3	0.0855	0.0859
1.723	3.339	3.02	0.085	0.0951
1.773	3.3395	3.08	0.0833	0.0695
1.8	3.4	3.110	0.0825	0.0685
1.82	3.41	3.12	0.0818	0.0745
1.85	3.42	3.13	0.0805	0.0973
1.90	3.425	3.15	0.078	0.112
1.935	3.45	3.19	0.076	0.0991
1.98	3.49	3.24	0.074	0.111
2	3.5	3.27	0.0735	0.119
2.04	3.53	3.27	0.0685	0.111
2.09	3.54	3.29	0.062	0.121
2.115	3.55	3.3	0.059	0.115
2.15	3.57	3.3	0.054	0.127
2.175	3.58	3.31	0.051	0.137
2.2	3.6	3.32	0.048	0.134
2.225	3.62	3.33	0.0445	0.136
2.275	3.64	3.36	0.0395	0.126
2.3	3.65	3.38	0.037	0.119
2.32	3.67	3.40	0.0345	0.115
2.35	3.69	3.42	0.032	0.111
2.4	3.73	3.45	0.0275	0.106

FIGURE CAPTIONS

1 - Comparison between calculated and experimental total neutron cross section

x [10]
o [11]
Δ [12]
— this work

2 - Cumulative level scheme of ^{232}Th.

3 - Calculated fission cross section compared to the experimental data :

● [16]
x † [1]
— this work

4 - Comparison between the calculated and experimental fission fragment angular distributions

o [2]
x [3]
— this work

5 - Fission cross section calculated by steps of 4 keV around E_n = 1.6 MeV.

6 - Angular distributions at neutron energies around E_n = 1.6 MeV

● experimental data [5]
--- calculated angular distribution with the assumption of a rotational band [5]
— this work

7 - Neutron elastic scattering cross section

— experimental evaluation [17]
--- this work

8 - Partial inelastic scattering cross sections

o● [18]
x [19]

Δ [17]

□ [20]

— this work

9 - Radiative capture cross section

x [21]

o [17]

● [22]

▲ [23]

□ [24]

— this work

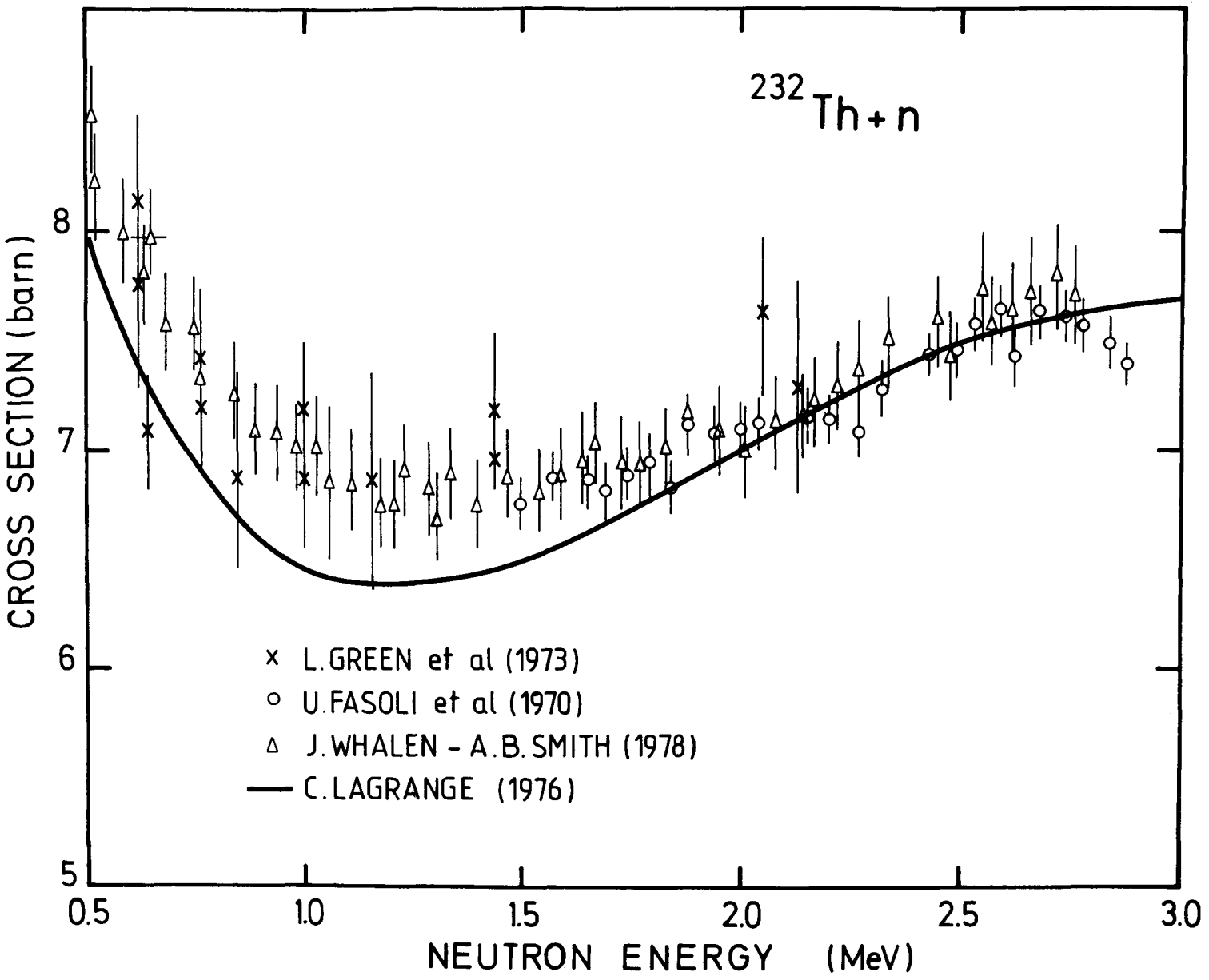
232 Th + n
CROSS SECTION (barn)
8
7
6
5
0.5
1.0
1.5
2.0
2.5
3.0
NEUTRON ENERGY (MeV)
× L.GREEN et al (1973)
○ U.FASOLI et al (1970)
△ J.WHALEN - A.B.SMITH (1978)
— C.LAGRANGE (1976)

Fig. 1

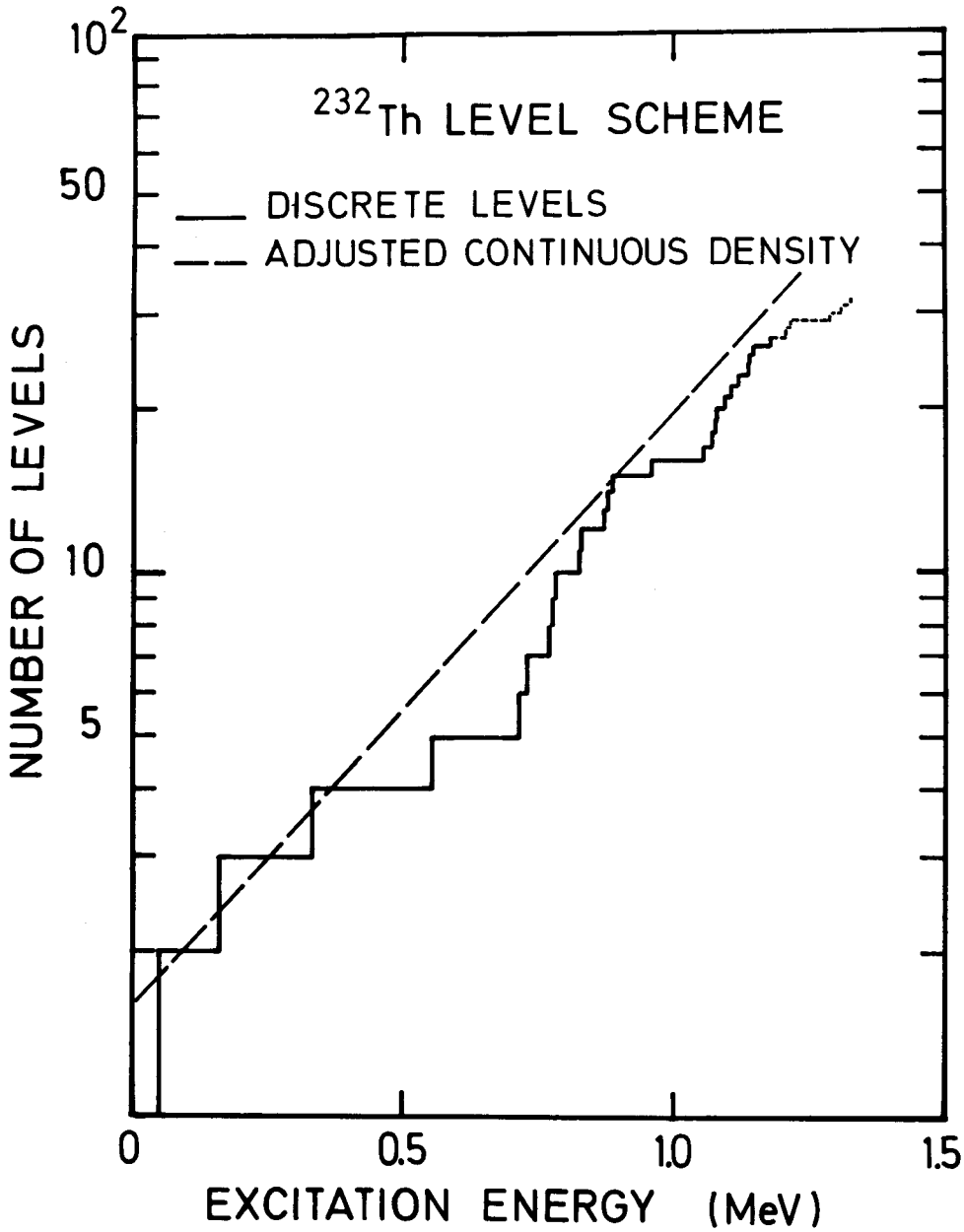
10^2
50
10
5
NUMBER OF LEVELS
^{232}Th LEVEL SCHEME
DISCRETE LEVELS
ADJUSTED CONTINUOUS DENSITY
0
0.5
1.0
1.5
EXCITATION ENERGY (MeV)

Fig. 2

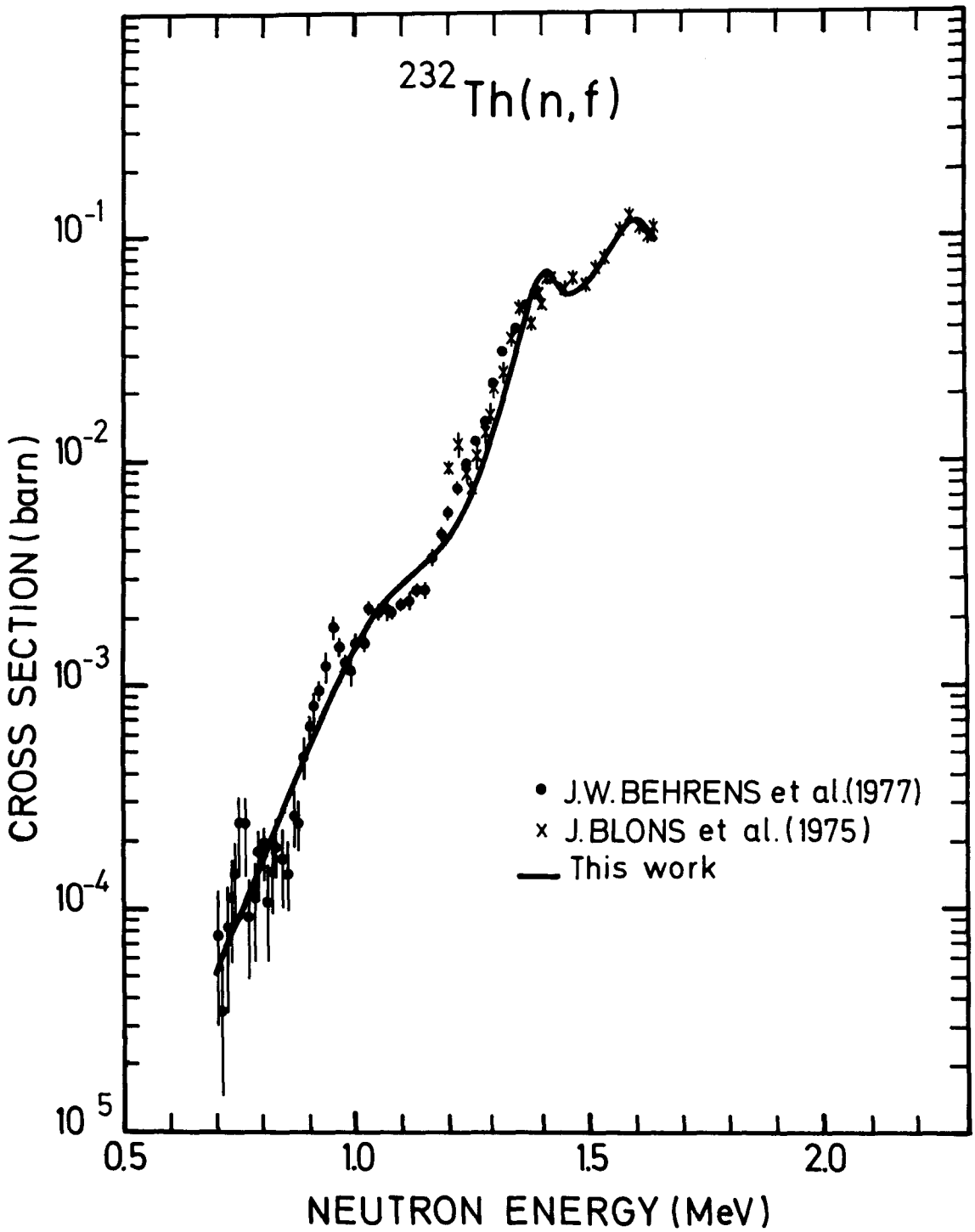
232Th(n,f)
CROSS SECTION (barn)
10-1
10-2
10-3
10-4
10 5
0.5
1.0
1.5
2.0
NEUTRON ENERGY (MeV)
• J.W. BEHRENS et al.(1977)
x J. BLONS et al. (1975)
This work

Fig. 3a

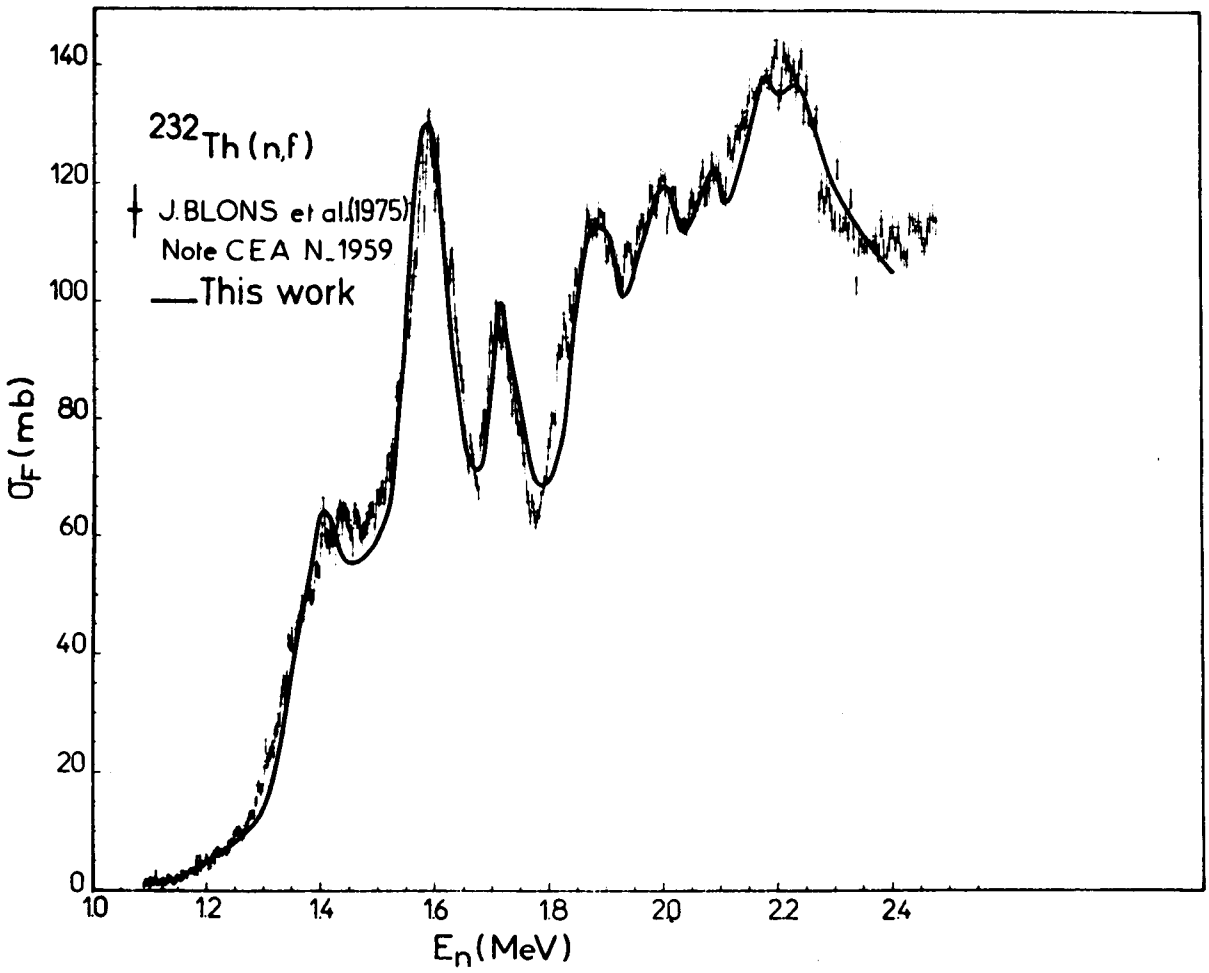
232Th (n,f)
J. BLONS et al.(1975)
Note CEA N_1959
This work
σF (mb)
En (MeV)
0
20
40
60
80
100
120
140
1.0
1.2
1.4
1.6
1.8
2.0
2.2
2.4

Fig. 3b

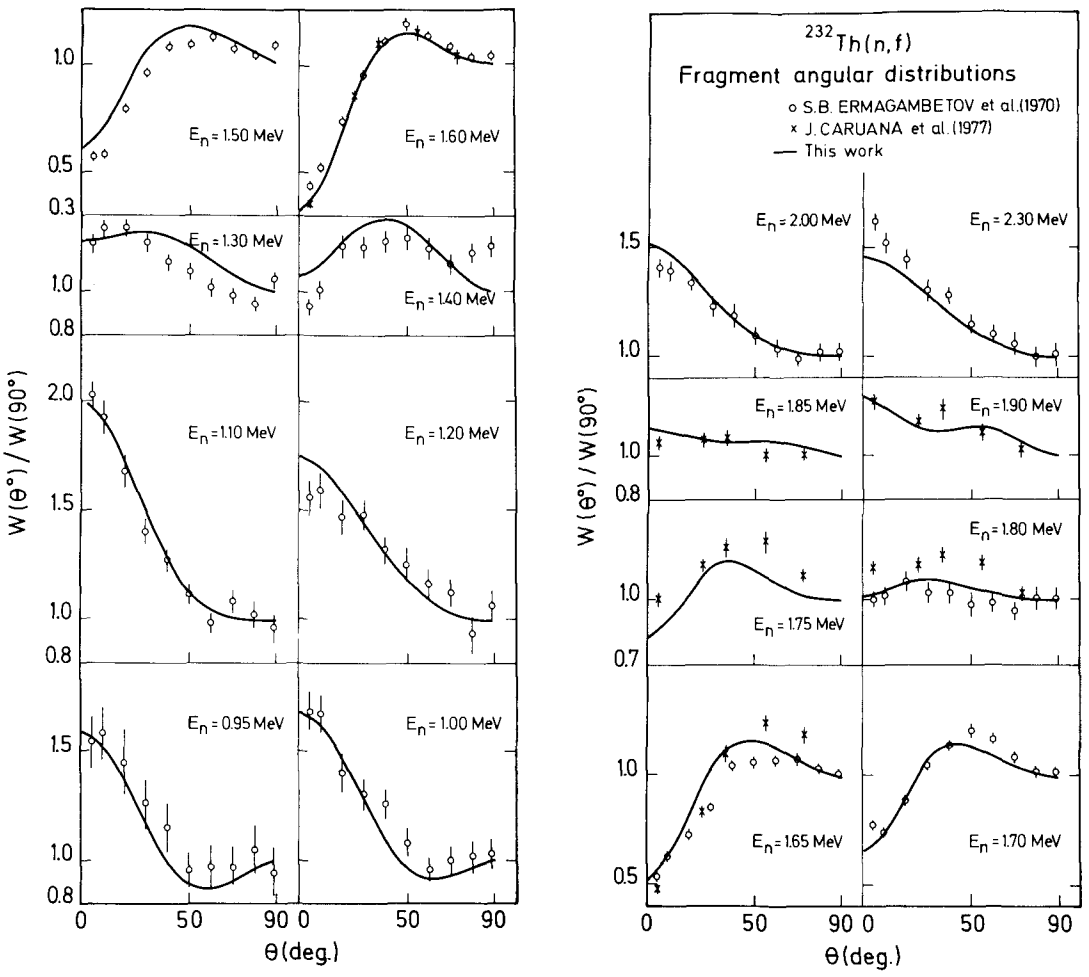
^{232}Th(n,f)
Fragment angular distributions
o S.B. ERMAGAMBETOV et al.(1970)
x J. CARUANA et al.(1977)
— This work
E_n = 1.50 MeV
E_n = 1.60 MeV
E_n = 1.30 MeV
E_n = 1.40 MeV
E_n = 1.10 MeV
E_n = 1.20 MeV
E_n = 0.95 MeV
E_n = 1.00 MeV
E_n = 2.00 MeV
E_n = 2.30 MeV
E_n = 1.85 MeV
E_n = 1.90 MeV
E_n = 1.80 MeV
E_n = 1.75 MeV
E_n = 1.65 MeV
E_n = 1.70 MeV
W(θ°) / W(90°)
θ(deg.)

Fig. 4

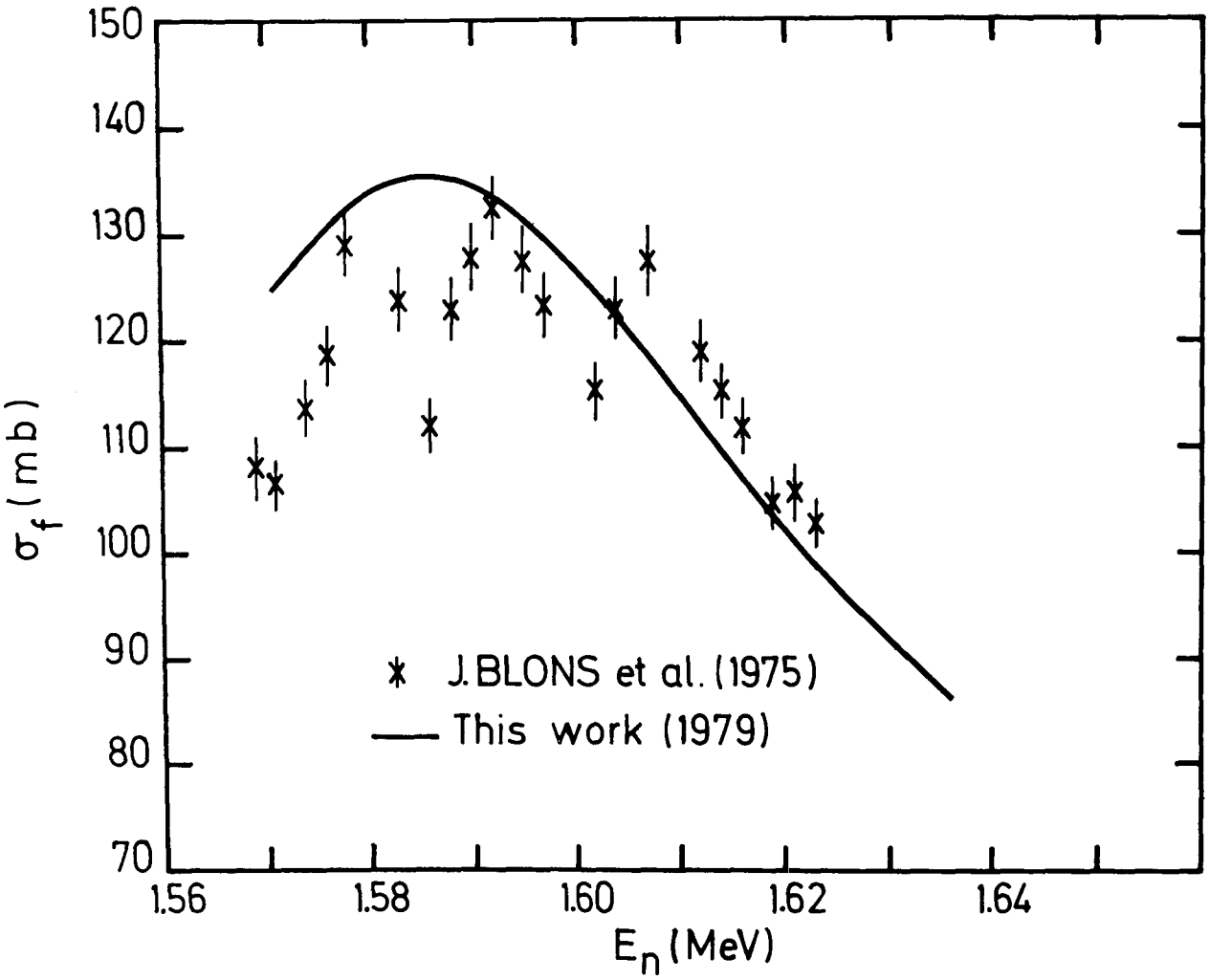
150
140
130
120
110
100
90
80
70
σ_f (mb)
1.56
1.58
1.60
1.62
1.64
E_n (MeV)
J. BLONS et al. (1975)
This work (1979)

Fig. 5

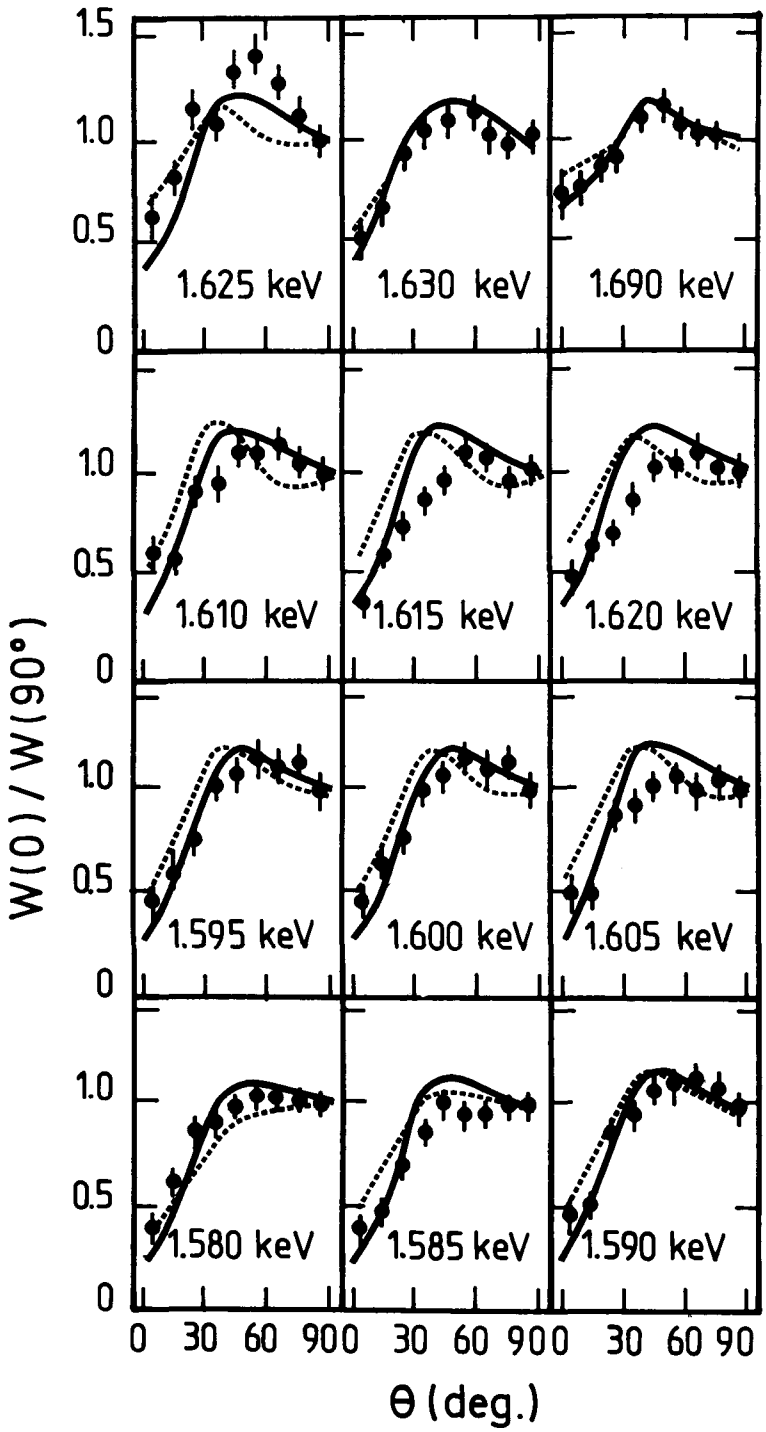
1.5
1.0
0.5
0
1.625 keV
1.630 keV
1.690 keV
1.610 keV
1.615 keV
1.620 keV
1.595 keV
1.600 keV
1.605 keV
1.580 keV
1.585 keV
1.590 keV
W(0) / W(90°)
0 30 60 90
θ (deg.)

Fig. 6

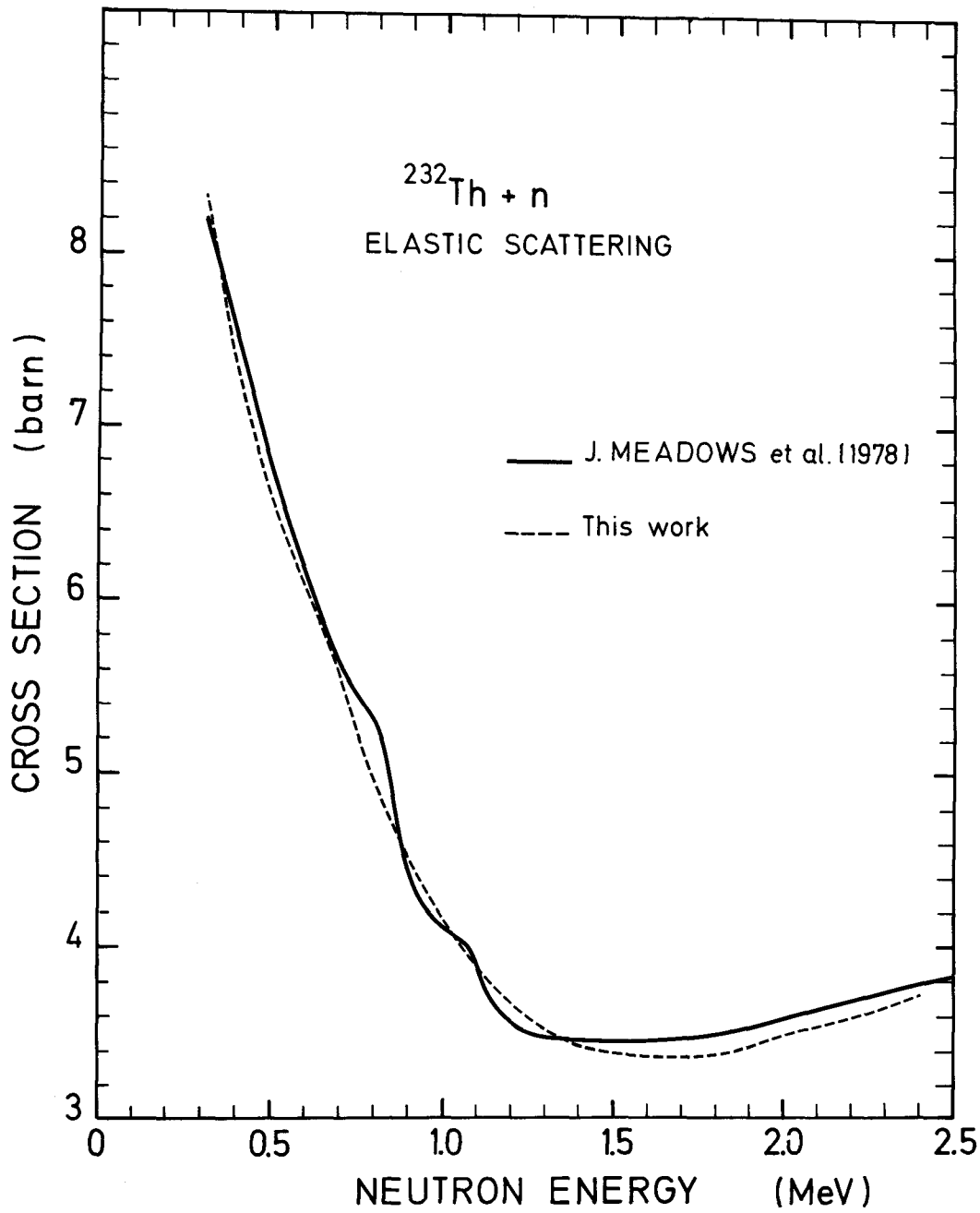
232Th + n
ELASTIC SCATTERING
J. MEADOWS et al. (1978)
This work
CROSS SECTION (barn)
NEUTRON ENERGY (MeV)
8
7
6
5
4
3
0
0.5
1.0
1.5
2.0
2.5

Fig. 7

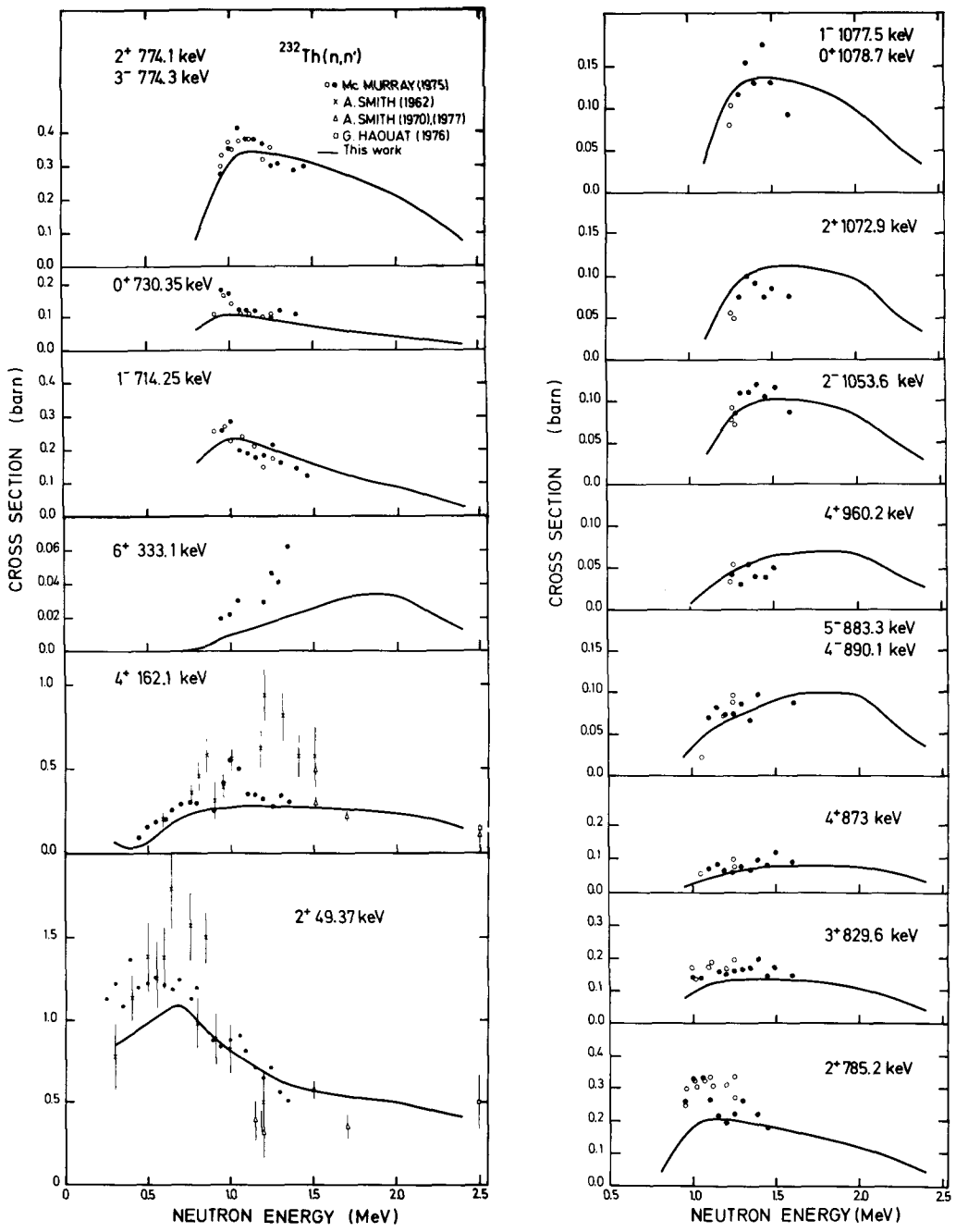
2+ 774.1 keV
3- 774.3 keV
232Th(n,n')
Mc MURRAY (1975)
A. SMITH (1962)
A. SMITH (1970),(1977)
G. HAOUAT (1976)
This work
0+ 730.35 keV
1- 714.25 keV
6+ 333.1 keV
4+ 162.1 keV
2+ 49.37 keV
CROSS SECTION (barn)
NEUTRON ENERGY (MeV)
1- 1077.5 keV
0+ 1078.7 keV
2+ 1072.9 keV
2- 1053.6 keV
4+ 960.2 keV
5- 883.3 keV
4- 890.1 keV
4+ 873 keV
3+ 829.6 keV
2+ 785.2 keV
CROSS SECTION (barn)
NEUTRON ENERGY (MeV)

Fig. 8

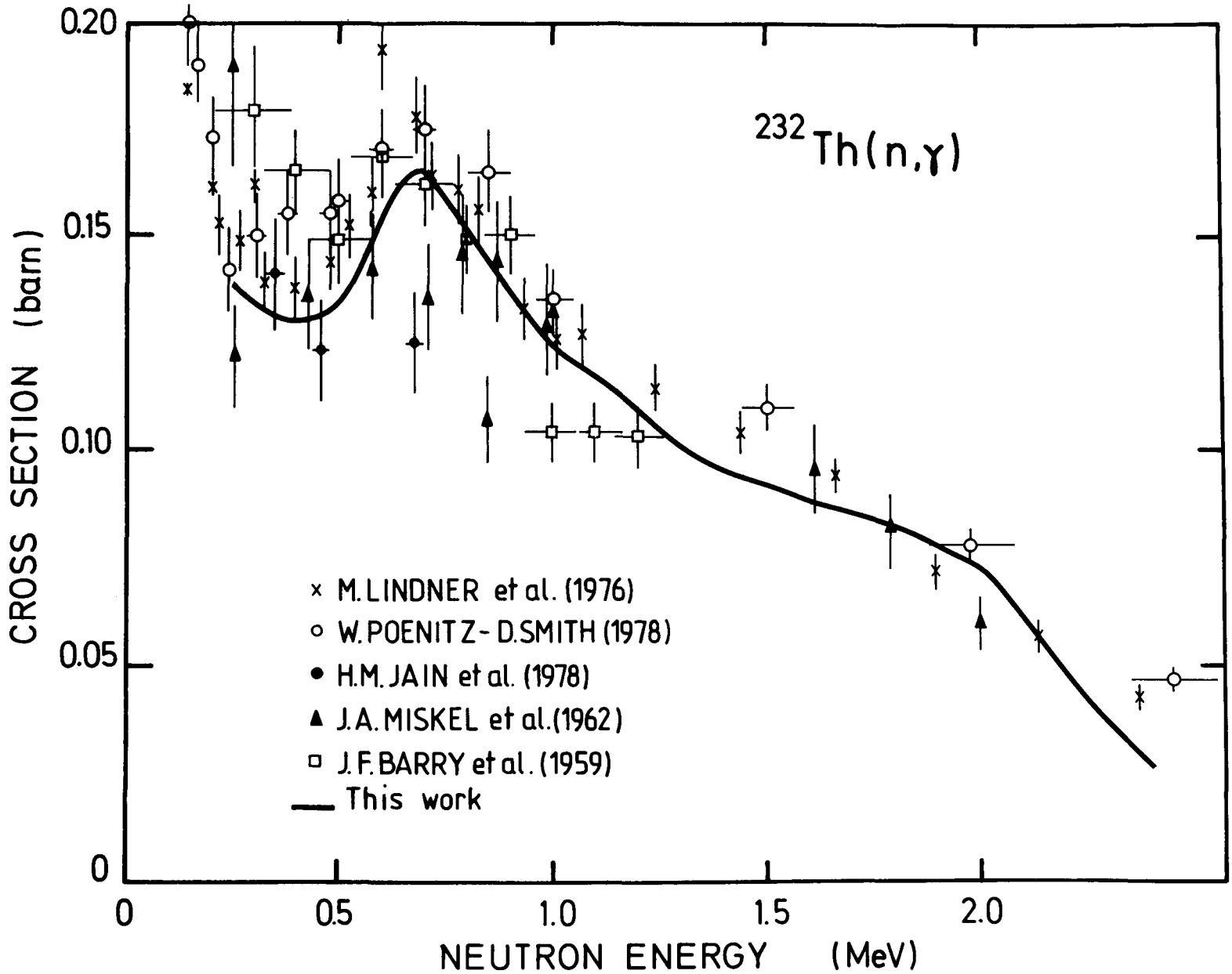
0.20
0.15
0.10
0.05
0
CROSS SECTION (barn)
0
0.5
1.0
1.5
2.0
NEUTRON ENERGY (MeV)
232Th(n,γ)
× M.LINDNER et al. (1976)
○ W.POENITZ-D.SMITH (1978)
● H.M.JAIN et al. (1978)
▲ J.A.MISKEL et al.(1962)
□ J.F.BARRY et al. (1959)
This work

Fig. 9